Polarization-dependent methanol adsorption on lithium niobate Z-cut surfaces

A. Riefer,* S. Sanna, and W. G. Schmidt
Lehrstuhl für Theoretische Physik, Universität Paderborn, 33095 Paderborn, Germany
(Received 29 April 2012; revised manuscript received 2 August 2012; published 6 September 2012)

The adsorption of single methanol molecules on the lithium niobate (0001) surface, commonly referred to as Z-cut, is investigated using first-principles calculations. It is found that the binding energy for molecular adsorption on the negative surface (∼1 eV) is about twice as large as for the positive surface. This difference is related to different bond strengths rather than electrostatics. Depending on the reaction path, lithium extraction from the negative surface may occur. This leads to an additional energy lowering by a few tenths of an eV. Larger energy gains are realized by dissociative adsorption, which is an activated process, however.

DOI: 10.1103/PhysRevB.86.125410 PACS number(s): 68.43.Bc, 77.84.Ek, 82.65.+r

I. INTRODUCTION

Due to its ferroelectric, piezoelectric, photorefractive, and electro-optical properties—reviewed, e.g., in Refs. 1,2—lithium niobate ($LiNbO_3$, LN) has become important in numerous areas of broad technological significance such as in modulators, wavelength filters, second-harmonic generators, and nonvolatile memories. These applications typically employ the LN bulk properties. In recent years, however, the LN surface and interface properties have found increasing interest. For example, encouraging GaN and also AlN growth results were obtained using LN substrates.[3–6] Thereby periodically polarized substrates can be used to spatially vary the GaN polarity.[7] This may be exploited for integrated electrical devices on lithium niobate.[8] Similarly, the ability to manipulate the dipole orientation in ferroelectric oxides has been suggested as a tool to tailor the surface reactivity for specific applications.[9] As ferroelectric domains can be patterned at the nanoscale, domain-specific surface chemistries may provide a method for fabrication of nanoscale devices. In fact, experiments with the adsorption of 2-propanol,[10] water as well as methanol,[11] and the anchoring of liquid-crystal molecules[12] indicate an influence of the surface poling on the adsorption characteristics.

While the typical mechanisms that are relevant for molecular adsorption on semiconductors and metals are basically understood, see, e.g., Ref. 13, only little is known on the details of the interaction between adsorbates and ferroelectric surfaces. The polarization-dependent adsorption characteristics observed in Refs. 10–12 have been tentatively attributed to various mechanisms such as charge transfer processes and/or electrostatic forces induced by space charge layers and band bending, external screening charges on the surface, the pyroelectric properties of the ferroelectric substrate, as well as the different atomic surface structure of oppositely polarized surfaces. A detailed microscopic understanding of how molecular species interact with LN surfaces is missing, however. Recently, microscopic models for the atomic structure of LN surfaces were proposed on the basis of first-principles calculations.[14,15] Based on these models, the present study aims at the better understanding of molecular adsorption phenomena on the polar LN(0001) surface, commonly referred to as Z-cut. Thereby methanol was chosen as the model adsorbate, due to its pronounced molecular dipole moment of about 1.7 D and the availability of experimental data.[9,11]

II. METHODOLOGY

In the present study first-principles projector augmented wave (PAW) calculations were performed using the VASP implementation of the density functional theory in the generalized gradient approximation (DFT-GGA).[16–18] In order to assess the influence of the electron exchange and correlation functional on the results, some calculations were also performed using the local density approximation (LDA).[19,20] Technically, the present study is on the same footing as our previous works on LN bulk[21] and surface properties.[15] The electron wave functions are expanded into plane waves up to an energy cutoff of 400 eV. The atomic structures of the differently polarized LN Z-cut surfaces were set up according to Refs. 14,15; i.e., we consider methanol adsorption on the positive (-Nb-O_3-Li_2 terminated) and negative (O-Li- terminated) LN(0001) surfaces shown schematically in Fig. 1. A dipole correction was applied along the surface normal in order to account for the sizable electric field. To minimize the interaction of the adsorbate molecules with respective images due to the usage of periodic boundary conditions, we employ a supercell that doubles the lateral dimensions of the surface unit cell in each direction. Material slabs consisting of 19/20 atomic layers were used to model the positive/negative surface. Along the surface normal a vacuum layer of 15 Å is used to separate the materials slabs including adsorbates. For the calculation of the potential energy surface (PES) and the investigation of the reaction path for the molecular dissociation, one special **k** point has been used to sample the surface Brillouin zone and the atomic coordinates were relaxed until the forces were lower than 0.05 eV/Å. The detailed investigation of the preferred adsorption configurations and the exploration of dissociative adsorption scenarios have been performed using a finer Γ centered $2\times2\times1$ **k**-point mesh and an upper limit of 0.02 eV/Å for the forces. The atomic positions in the bottom layers of the slab were frozen in ideal bulk positions during the structural relaxation, while the upper three (five) layers of the positive (negative) surface as well as the adsorbate were freely relaxed. Test calculations with $2\times2\times2$, $3\times3\times1$, $3\times3\times2$, $4\times4\times1$, and $4\times4\times2$ **k**-point samplings, an increased vacuum layer of up to 35 Å, and thicker materials slabs containing up to 42 layers were performed in order to determine the numerical accuracy of the present results. Error bars of 0.05 eV for the adsorption energies and 0.01 Å for atomic distances are concluded from these tests.

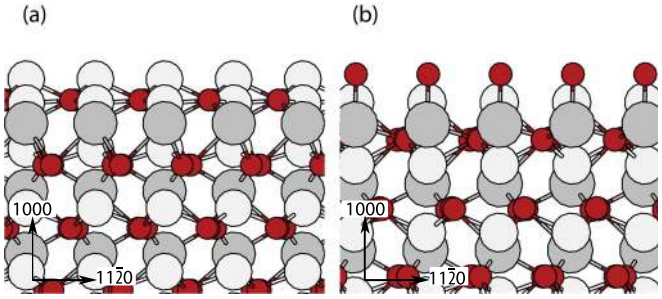

FIG. 1. (Color online) Side view of the stable positive (a) (-Nb-O_3-Li_2 terminated) and negative (b) (O-Li- terminated) LN(0001) surface. White, gray, and small circles denote Li, Nb, and O atoms, respectively.

III. RESULTS AND DISCUSSION

At first the potential energy surface (PES) is calculated in order to identify the most favorable adsorption sites and adsorption configurations of single methanol molecules on LN. Thereby we used a mesh of 48 nearly equidistant lateral points to probe the local binding energy due to adsorption

$$E_B = E(\text{Meth}) + E(\text{Surface}) - E(\text{Meth} + \text{Surface}), \qquad (1)$$

where E(Meth), E(Surface), and E(Meth + Surface) are the total energies of the isolated molecule in gas phase, the clean LN surface, and the energy of the adsorption structure, respectively. In the PES calculations, the lateral position of the molecular oxygen is fixed, but the remaining degrees of freedom are relaxed. Eight different starting configurations (see Fig. 2) are probed for each point of the lateral mesh, in order to reduce the probability that the system gets trapped in metastable configurations. Thus, altogether 384 starting configurations had to be probed for each surface. The initial height of the oxygen atom was chosen to be $2.6/3.0 \pm 0.2$ Å above the uppermost atom of the positive/negative surface. The lowest energy configuration obtained from the various starting geometries for each mesh point is then used to map the PES.

The resulting energy landscapes for the positive and negative LN surfaces are shown in Fig. 3. In the case of the positive surface, the calculations yield binding energies ranging from values close to zero to about 0.5 eV. Methanol strongly prefers to adsorb close to the surface oxygen atoms. Three pronounced energy minima of the energy surface (A, B, and C) are indicated by arrows. The corrugation of the PES is more pronounced on the negative surface. Here the

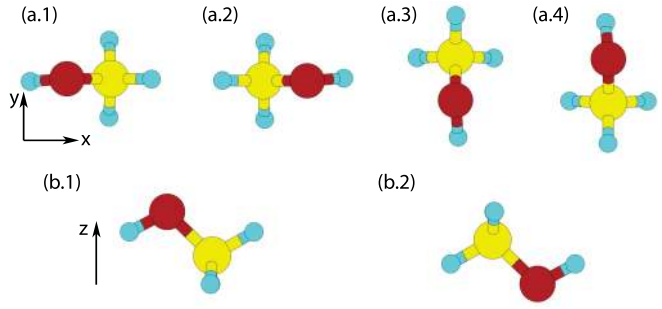

FIG. 2. (Color online) Schematic view of the eight different methanol starting orientations used in the PES calculation. See text.

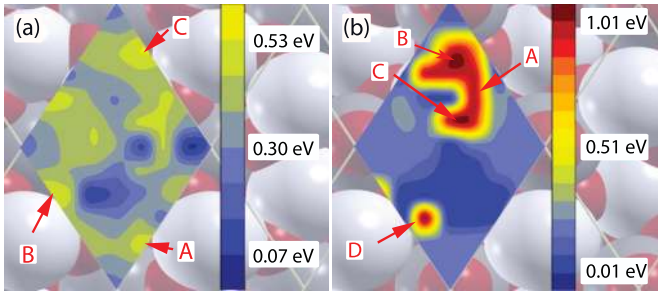

FIG. 3. (Color online) Calculated potential energy surfaces for the adsorption of methanol on the positive (a) and negative (b) LN surface. The primitive surface unit cell used is indicated.

binding energies vary between essentially zero and 1 eV. Four pronounced energy minima [A, B, C, and D in Fig. 3(b)] occur for molecular adsorption positions close to surface lithium.

The adsorption configurations corresponding to pronounced energy minima on the PES of the positive and negative Z-cut surfaces were used as starting configurations for a full structural relaxation without any geometrical constraint. The slightly increased binding energies for the respective configurations A, B, and C are compiled in Table I.

The geometry of the energetically most favored bonding configuration (A) of methanol on the positive and negative surface is shown in Figs. 4(a) and 4(b), respectively. In order to elucidate the bonding mechanism, the difference of the charge densities of the adsorption structure and the isolated clean surface and gas-phase molecule (both in the geometry of the adsorption structure) is calculated. The result is shown in Figs. 5(a) and 5(b) for the positive and negative LN Z-cut surface, respectively. On the positive surface, the molecular hydroxyl group hydrogen H_M points towards a surface oxygen O_S. As seen in Fig. 5(a), there is indeed a charge accumulation between H_M and O_S. However, charge accumulates also between the molecular oxygen O_M and surface lithium Li_S. The H_M-O_S and O_M-Li_S distances amount to 1.8 and 2.1 Å. Similar values are obtained for the bonding configurations B and C on the positive surface; see Table I. This indicates a weak hydrogen bond between the molecular hydroxyl group and the surface oxygen as well as a covalent interaction between the molecular oxygen and surface lithium. In order to better understand the energetics of the methanol adsorption, we also calculated the molecular and surface deformation energies. While the molecular strain is negligible, the deformation of the surface costs about 0.1 eV in case of the bonding configuration A. Again, the situation is similar for the geometries B and C of the positive surface; see Table I.

Test calculations performed within DFT-LDA rather than using the GGA for the adsorption configuration A result—as expected due to the overbinding typical for LDA—in stronger adsorption energies (0.91/1.37 eV for the positive/negative surface) and shorter bond lengths. The O_M-Li_S distances are reduced, for example, by 0.07/0.08 Å for the positive/negative surface. Despite these noticeable changes, the change of the *energy difference* between adsorption on the two surface polarizations is remarkably small: Adsorption on the negative surface is preferred by 0.46 eV within the LDA, very close to the GGA value of 0.45 eV. Therefore we expect the conclusions

TABLE I. Selected properties for the most favored configurations A, B, and C (see Fig. 3) of methanol on the positive and negative LN(0001) surfaces. Given are the binding energies E_B, the strain energies E_{ss} and E_{sm} due to the deformation of the surface and the molecule, respectively, the molecular dipole component parallel to the surface normal p_z, and the O_M-Li_S and H_M-O_S distances. Energies are given in eV, dipole moments in D, and lengths in Å.

	Positive Surface						Negative Surface					
Configuration	E_B	$d(O_M\text{-}Li_S)$	$d(H_M\text{-}O_S)$	E_{ss}	E_{sm}	p_z	E_B	$d(O_M\text{-}Li_S)$	$d(H_M\text{-}O_S)$	E_{ss}	E_{sm}	p_z
A	0.57	2.07	1.82	0.14	0.01	−0.19	1.02	1.87	1.73	0.06	0.04	1.25
B	0.56	2.05	1.84	0.14	0.02	−0.24	1.02	1.87	1.74	0.06	0.03	1.25
C	0.51	2.04	2.05	0.04	0.00	−0.24	1.01	1.87	1.75	0.09	0.04	1.25

from our study to be robust with respect to the treatment of the electron exchange and correlation energy.

The spontaneous surface polarization charge density of the ideal, bulk-truncated LN Z-cut amounts to $\sigma = 0.7$ C/m^2 (see Ref. 22). Given this value, a sizable contribution of electrostatic interactions to the interface energetics may be expected. However, on real surfaces considerably smaller surface charges are measured, due to various charge compensation mechanisms.[23] Johann and Soergel[24] recently measured a value of $\sigma = 140$ μC/m^2 for congruently melted, undoped z-faced $LiNbO_3$ crystals under ambient conditions. This value is likely to contain in addition to internal charge compensation mechanisms also contributions from molecular adsorbates such as water from the ambient. From the charge density calculated self-consistently in this work we determine a value of $\sigma = 600$ μC/m^2 for the macroscopic surface charge of the atomically clean, structurally relaxed LN Z-cut. This value is in between the estimate from the bulk polarization and the value measured in ambient conditions. This can be expected, as the surface polarization charge is partially compensated by a stoichiometric change of the surface termination (internal compensation) and partially compensated by adsorbates (external compensation). Only the former effects are included in our calculations. The maximum change of the potential energy of the methanol molecular dipole moment in the electric field due the surface charge density calculated here allows for determining the upper limit for the contribution of surface charge polarization to the difference in methanol binding energies for the two surface orientations. We obtain a value of less than 3 meV, which is insignificant compared to the energies released upon covalent bond formation. The actual influence of the surface polarization on the interface energetics is even smaller, as can be seen from the calculated molecular dipole moments parallel to the surface normal compiled in Table I.

Summarizing the results so far, we find that there are three rather similar adsorption configurations A, B, and C on the positive surface that yield a binding energy of about 0.5 eV. This energy is dominated by the chemical interaction between surface oxygen and lithium atoms with molecular hydrogen and oxygen, respectively. The adsorption configurations do not involve substantial strain in either the molecule or the substrate. The electrostatic interaction between the molecular dipole and the surface polarization charge does not contribute substantially to the interface energetics. Molecular adsorption is substantially more favorable on the negative surface. Here the favored bonding configurations A, B, and C (see Fig. 3) result in binding energies larger than 1 eV (see Table I). The corresponding bonding scenarios are similar to the ones on the positive surface, i.e., molecular oxygen and hydoxyl-group hydrogen bond to surface lithium and oxygen atoms. The difference in adsorption energy between negative and positive surface is mainly due to stronger bonds in the former case. This is reflected in shorter bonds—the bond distances $d(H_M\text{-}O_S)$ and $d(O_M\text{-}Li_S)$ are shorter by 0.1–0.3 Å—as well as by an increased charge accumulation between the respective atoms as shown in Fig. 5. Similarly to the adsorption on the positive Z-cut, strain and electrostatic contributions to the adsorption energetics are comparatively minor.

The adsorption configuration corresponding to the position D on the negative surface [see Fig. 3(b)] has not been discussed so far. This very favorable adsorption structure is related to the extraction of a surface lithium (denoted Li_D in Fig. 6) that subsequently bonds to the methanol oxygen. The corresponding modification of the LN surface depends sensitively on the reaction path and starting configuration. If

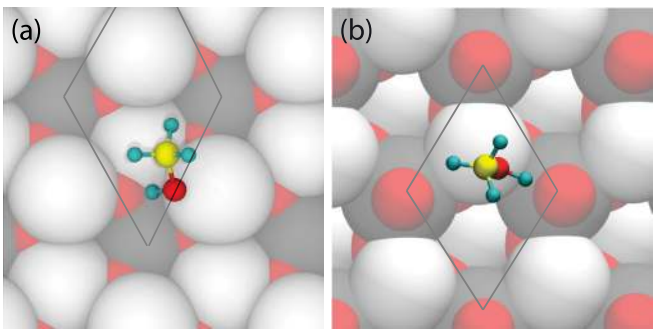

FIG. 4. (Color online) Top view of the relaxed bonding configuration A on the positive (a) and negative (b) LN surface (see text). The primitive surface unit cell is indicated.

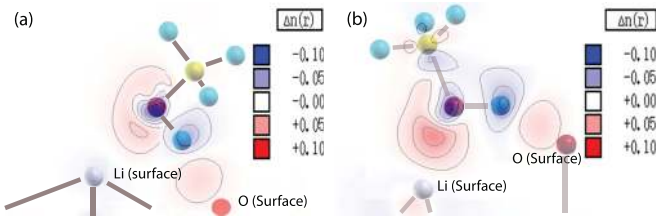

FIG. 5. (Color online) Calculated charge-density difference (in e/Å^3) of the methanol bonding configuration A on the positive (a) and negative (b) LN surface.

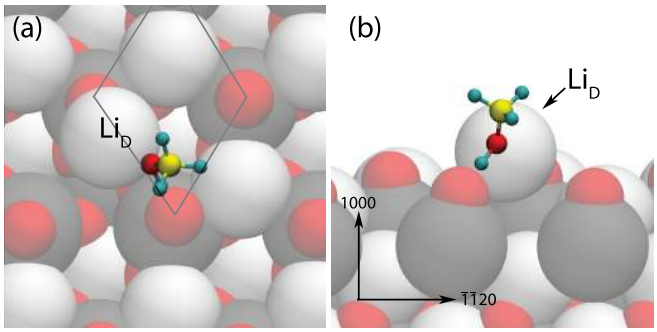

FIG. 6. (Color online) Top view (a) and side view (b) of the adsorption configuration D on the negative LN surface (see text). The surface extracted Li_D atom is marked.

no geometrical constraints are applied, the system gets trapped in a metastable configuration instead. In order to investigate this effect more systematically and detect possible further adsorption (physisorption) configurations that may occur in addition to the relatively strong chemisorbed bonding situations discussed above, we calculate the energy as a function of the molecule-surface distance. Thereby the molecular oxygen is laterally fixed and moved vertically, while all other atoms are free to relax. The calculated energies (for the adsorption sites A, B, and C) are shown in Figs. 7(a) and 7(b) for the case of the positive and negative surface, respectively. In neither case are activation barriers hindering the adsorption found. For the positive surface a single energy minimum for the adsorption height of about 1.5 Å is found. In case of the negative Z-cut a second pronounced energy minimum at a distance of about 1.6 Å for the adsorption configurations A and B is found in addition to the energy minimum at about 0.7 Å that occurs for all three adsorption configurations In these cases, similarly to the configuration D discussed above, a lithium atom is extracted from the surface and bonds to the adsorbate. Again, we find the formation of these structures that are accompanied by a partial surface rearrangement to be highly dependent on

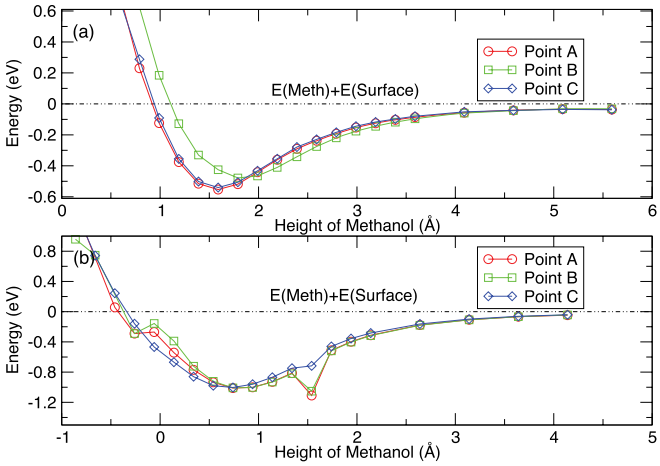

FIG. 7. (Color online) Calculated energy vs molecule-surface distance (given with respect to the uppermost surface atom) for the adsorption configurations A, B, and C on the positive (a) and negative (b) LN surface. The energy of the state describing the isolated molecule and surface is set to zero.

the details of the reaction path. In any event, the calculations indicate that the molecular adsorption on the negative Z-cut is more likely to lead to an extraction of surface atoms than adsorption on the positive surface. This corresponds to the finding that the atomic bonds on the negative surface are softer than on the positive LN surface, as concluded from the surface vibrational properties (see Ref. 25): The vertical surface Li mode on the positive Z-cut, e.g., is blueshifted by 61 cm^{-1} with respect to its counterpart on the negative surface. The present finding of a rather different surface chemistry of oppositely polarized LN surfaces towards methanol agrees with earlier reports on other molecular species. For example, the different etching rate of $LiNbO_3$ or $LiTaO_3$ surfaces using HF and HNO_3 acid mixtures is exploited to visualize ferroelectric domains.[26–28]

It is not only possible that the LN surface gets partially destructed due to the adsorption process; also the molecule may dissociate. Here we probed the dissociation of methanol into a methyl and a hydroxyl group that bond separately on the surface. Different starting configurations on surface oxygen were probed for the methyl group, whereas the hydroxyl group bonds to a surface lithium. While the separation into CH_3 and OH groups leads to a stable configuration on the negative surface, a rearrangement into hydroxymethyl (H_2COH) and hydrogen or water and methylene (CH_2) is found to lower the total energy even further (by nearly 2 eV) on the positive surface. In the first case, the hydrogen attaches to a surface oxygen while the carbon and the oxygen of the hydroxymethyl group bonds to a surface oxygen and lithium, respectively. Water adsorbs close to surface lithium and methylene bonds between two surface oxygens. On the negative LN Z-cut dissociation into methyl and hydroxyl groups is most favorable. In agreement with calculations by Hölscher *et al.*,[29] the hydroxyl group is found to bond between lithium and niobium, while the methyl group bonds to surface oxygen. All dissociation processes lead to a strong modification of the surface, as indicated by the huge strain energies E_{ss} of about 1.3–2.0 eV (see Table II), since the newly arising bonds with the fragments A and B strongly modify the atomic structure of the LN substrate.

The calculated energies

$$E_D = E(\text{Surface}) + E(\text{Meth}) - E(\text{Surface} + \text{A} + \text{B}), \qquad (2)$$

where $E(\text{Surface} + \text{A} + \text{B})$ denotes the energy of the surface with the molecular fragments A and B adsorbed, are compiled in Table II. Obviously, compared to the nondissociative adsorption, a substantial energy gain results from the

TABLE II. Energetics (in eV) of dissociative adsorption reactions (see text and Fig. 9 for details). E_{act} and E_{ss} denote the activation energy and the strain energy due to the deformation of the surface.

	Positive Surface		Negative Surface
A + B	$H_2COH + H$	$H_2O + CH_2$	$CH_3 + OH$
E_{act}	≈4.5	≈6.4	≈2.4
E_D	2.27	2.53	1.34
E_{ss}	1.92	1.99	1.29

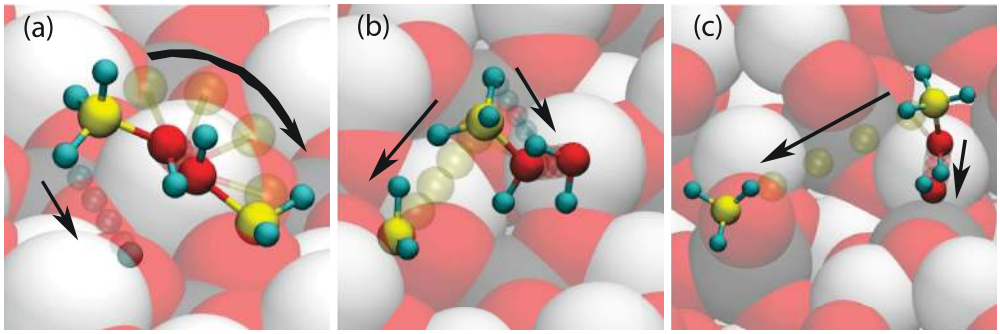

FIG. 8. (Color online) Sketches of (intermediate) geometries of the reactions (a) $CH_3OH \rightarrow H_2COH + H$, (b) $CH_3OH \rightarrow H_2O + CH_2$ on the positive LN surface, and (c) $CH_3OH \rightarrow CH_3 + OH$ on the negative surface. The atom positions of the intermediate geometries are light. Only the moving hydrogen, the carbon, and the oxygen are shown.

molecular fragmentation on the surface. In order to explore the probability for dissociative adsorption, approximate activation energies were calculated. Thereby we perform constrained dynamics calculations starting from the various dissociative adsorption configurations. Intermediate states were created by interpolation from the initial and final atomic geometries; see Figs. 8(a)–8(c). In the case of the $CH_3OH \rightarrow H_2COH + H$ reaction on the surface, the movement of the C-O group was assumed to be a rotation coupled with a translation, as shown in Fig. 8(a). Hydrogen attached to carbon or oxygen was allowed to fully relax for each step on the reaction path in the case of reactions on the negative surface. In the case of the positive surface the transferred hydrogen (either from the methyl to the hydroxyl group or from the methyl group to the surface) was fixed in the intermediate states. The calculated energies along the reaction paths are shown in Fig. 9. While the dissociative adsorption is more favored on the positive than on the negative surface (see Table II), it is found that also the activation energies are considerably larger for the positive than for the negative surface. Considering the energies compiled in Table II, a word of caution is in order. On the one hand, the number of conceivable configurations exceeds by far the number of structures that can be probed computationally. Thus, configurations that are even more favorable than the ones found here cannot be excluded. On the other hand, the calculated energy barriers are by construction upper limits for the actual activation energies. Proton quantum effects can be expected to further lower the energy barriers.[30] Given the considerable barriers calculated here, their influence can be considered to be minor though.

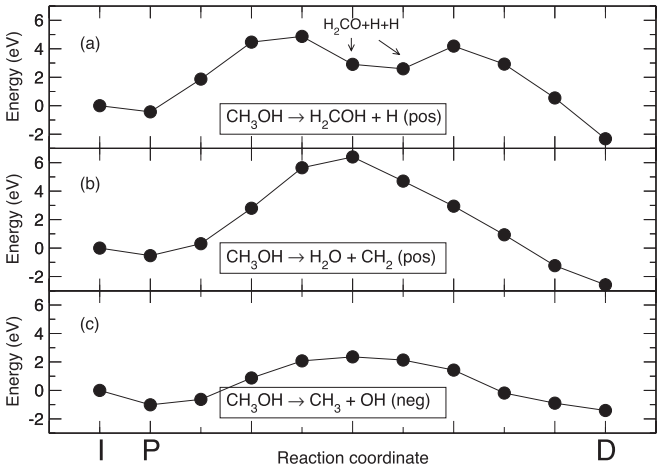

FIG. 9. Energetics of dissociative surface reactions of methanol on the positive [(a), (b)] or negative (c) LN surface. I, P, and D denote the state of the isolated molecule and surface, the interacting but intact (physisorbed), and the dissociated molecule on the surface.

The present finding that the dissociative adsorption is an activated process with a considerable barrier agrees with temperature programmed desorption (TPD) measurements by Garra *et al.*[11] that concluded on a molecular desorption of methanol from the surface. They found the desorption temperature of methanol to be both coverage and polarization dependent. In the zero-coverage limit they determined—assuming pre-exponential factors of 10^8 and 10^{13} s^{-1}, respectively—binding energies of 0.58/0.61 eV and 0.88/0.93 eV for the positive/negative LN Z-cut. (Here it should be pointed out that a convention different from the present one has been used in Ref. 11 to discriminate between the positive and negative surface.) The calculated and measured binding energies roughly agree concerning the order of magnitude. Also, the measured increase of the binding energy by going from the positive to the negative surface is in agreement with the present calculations. However, experimentally an increase of about 30–50 meV has been found, while the calculations predict a difference of nearly 0.5 eV. Possibly the surface termination of the real substrate differs from the one assumed in our calculations. In particular thin films of additional adsorbates may modify the molecular adsorption mechanism. For more definite conclusions a thorough surface characterization of the ferroelectric samples on the atomic scale would be helpful.

IV. SUMMARY

In summary, DFT-GGA calculations on the adsorption of single methanol molecules on LN Z-cut surfaces were presented. In the case of molecular adsorption, the hydroxyl group hydrogen bonds to surface oxygen and molecular oxygen bonds to surface lithium, both for adsorption on the positive and the negative Z-cut. Despite the similar adsorption configurations a remarkable difference in the adsorption energetics for the positive and negative surface is found.

Adsorption is clearly more favorable on the negative surfaces, with binding energies of about 1 eV in comparison to about half an eV gained upon adsorption on the positive Z-cut. This difference is due to stronger chemical bonds rather than related to the different surface polarization charge of the ferroelectric substrate. Also strain plays only a minor role for the adsorption energetics. Molecular fragmentation leading to dissociative adsorption configurations is an activated process that lowers the energy (with respect to molecular adsorption) on both the positive and the negative Z-cut. The negative LN surface is susceptible to lithium extraction upon methanol adsorption. The present results indicate that the experimentally observed higher etching rate of the negative surface with respect to specific acids is an expression of a higher surface reactivity in general. This difference in reactivity, however, is related to the difference in atomic structure and stoichiometry of the two polarizations rather than to the surface charge of the related macroscopic surface electric field itself.

ACKNOWLEDGMENTS

We thank the Deutsche Forschungsgemeinschaft for financial support. The calculations were done using grants of computer time from the Paderborn Center for Parallel Computing (PC^2) and the Höchstleistungs-Rechenzentrum Stuttgart.

*Corresponding author: riefer@mail.uni-paderborn.de

[1] A. Räuber, Curr. Top. Mater. Sci. **1**, 481 (1978).
[2] R. S. Weis and T. K. Gaylord, Appl. Phys. A **37**, 191 (1985).
[3] Y. Tsuchya, A. Kobayashi, J. Ohta, H. Fujioka, and M. Oshima, Jpn. J. Appl. Phys. **44**, L1522 (2005).
[4] Y. Tsuchya, A. Kobayashi, J. Ohta, H. Fujioka, and M. Oshima, Phys. Status Solidi A **202**, R145 (2006).
[5] Y. Tsuchya, A. Kobayashi, J. Ohta, H. Fujioka, and M. Oshima, J. Cryst. Growth **293**, 22 (2006).
[6] Y. Tsuchya, M. Oshima, A. Kobayashi, J. Ohta, and H. Fujioka, J. Vac. Sci. Technol. A **202**, 2021 (2006).
[7] W. A. Doolittle, G. Namkoong, A. G. Carver, and A. S. Brown, Solid-State Electron. **47**, 2143 (2003).
[8] G. Namkoong, K.-K. Lee, S. M. Madison, W. Henderson, S. E. Ralph, and W. A. Doolittle, Appl. Phys. Lett. **87**, 171107 (2005).
[9] D. Li, M. H. Zhao, J. Garra, A. M. Kolpak, A. M. Rappe, D. A. Bonnell, and V. J. M, Nat. Mater. **7**, 473 (2008).
[10] Y. Yun, L. Kampschulte, M. Li, D. Liao, and E. I. Altman, J. Phys. Chem. C **111**, 13951 (2007).
[11] J. Garra, J. M. Vohs, and D. A. Bonnell, Surf. Sci. **603**, 1106 (2009).
[12] S. C. Bharath, K. R. Pimputkar, A. M. Pronschinske, and T. P. Pearl, Appl. Surf. Sci. **254**, 2048 (2008).
[13] W. G. Schmidt, K. Seino, M. Preuss, A. Hermann, F. Ortmann, and F. Bechstedt, Appl. Phys. A **85**, 387 (2006).
[14] S. V. Levchenko and A. M. Rappe, Phys. Rev. Lett. **100**, 256101 (2008).
[15] S. Sanna and W. G. Schmidt, Phys. Rev. B **81**, 214116 (2010).
[16] G. Kresse and J. Furthmüller, Comput. Mater. Sci. **6**, 15 (1996).
[17] G. Kresse and D. Joubert, Phys. Rev. B **59**, 1758 (1999).
[18] J. P. Perdew, J. A. Chevary, S. H. Vosko, K. A. Jackson, M. R. Pederson, D. J. Singh, and C. Fiolhais, Phys. Rev. B **46**, 6671 (1992).
[19] D. M. Ceperley and B. J. Alder, Phys. Rev. Lett. **45**, 566 (1980).
[20] J. P. Perdew and A. Zunger, Phys. Rev. B **23**, 5048 (1981).
[21] W. G. Schmidt, M. Albrecht, S. Wippermann, S. Blankenburg, E. Rauls, F. Fuchs, C. Rödl, J. Furthmüller, and A. Hermann, Phys. Rev. B **77**, 035106 (2008).
[22] *Ferroelectrics and Related Substances: Oxides,* edited by K.-H. Hellwege and A. M. Hellwege, Landolt-Börnstein, New Series, Group III, Vol. 16, Pt. A (Springer-Verlag, Berlin, 1981).
[23] T. Jungk, Á. Hoffmann, and E. Soergel, Appl. Phys. Lett. **89**, 042901 (2006).
[24] F. Johann and E. Soergel, Appl. Phys. Lett. **95**, 232906 (2009).
[25] S. Sanna, G. Berth, W. Hahn, A. Widhalm, A. Zrenner, and W. G. Schmidt, IEEE Transactions Ultrasonics, Ferroelectrics, Frequency Control **58**, 1751 (2011).
[26] X. Liu, K. Terabe, M. Nakamura, S. Takekawa, and K. Kitamura, J. Appl. Phys. **97**, 064308 (2005).
[27] K. Nassau, H. J. Levinstein, and G. M. Loiacono, Appl. Phys. Lett. **6**, 228 (1965).
[28] N. Argiolas, M. Bazzan, A. Bernardi, E. Cattaruzza, P. Mazzoldi, P. Schiavuta, C. Sada, and U. Hangen, Mater. Sci. Eng. B **118**, 150 (2005).
[29] R. Hölscher, S. Sanna, and W. G. Schmidt, Phys. Status Solidi C **9**, 1361 (2012).
[30] J. Morrone and R. Car, Phys. Rev. Lett. **101**, 017801 (2008).